Viscous Compressible and Incompressible Flow in Slender Channels†

JAMES C. WILLIAMS III*
North Carolina State College

Summary

An analytical study is made of viscous flow in slender channels. Similar solutions to the approximate equations of motion, valid for flow at moderate or high Reynolds numbers in slender channels, are found for incompressible two-dimensional and axisymmetric flows and for compressible flows through two-dimensional channels with adiabatic walls. A study of compressible flows in convergent-divergent channels yields results regarding the effect of viscosity on the location of the sonic line, on the pressure ratio at the geometric throat and on the discharge coefficient for such channels.

Symbols

a,b = constants
cp = specific heat at constant pressure
$cn(\omega,k)$ = cosine amplitude u; Jacobian elliptic function
$dn(\omega,k)$ = delta amplitude u; Jacobian elliptic function
f = nondimensional stream function
$F(\phi,k)$ = incomplete elliptic integral of the first kind
F_x,F_y = body forces in x and y direction respectively
g^* = nondimensional velocity variable
h = nondimensional velocity variable
k = thermal conductivity of the gas, also modulus of the elliptic functions
L = characteristic length in the x-direction
$\dot{m}$ = mass flow through the channel
M = Mach number
p = pressure
Q = energy addition to the gas stream
R = wall coordinate in transformed compressible flow problem
$\mathfrak{R}$ = gas constant
Re = Reynolds number
$sd(\omega,k)$ = $sn(\omega,k)/dn(\omega,k)$
$sn(\omega,k)$ = sine amplitude u; Jacobian elliptic function
T = temperature
u,v = longitudinal and transverse velocity components
U,V = transformed longitudinal and transverse velocity components
x,y = longitudinal and transverse coordinates
X,Y = transformed longitudinal and transverse coordinates
α,β = constants
γ = ratio of specific heats
ϵ = 1 or 0 for axisymmetric or two-dimensional flow respectively
η = nondimensional transverse coordinate
μ = coefficient of viscosity
ν = coefficient of kinematic viscosity
ξ = nondimensional longitudinal coordinate
ρ = mass density
ψ = stream function

Subscripts

0 = stagnation conditions
1 = conditions at $x = 0$
t = conditions at the geometric throat

Received by IAS August 22, 1962. Revised and received October 25, 1962.

† Supported by the Air Force Office of Scientific Research and the Office of Naval Research under contract AF 49(638)-831.

* Associate Professor, Mechanical Engineering, formerly Research Scientist, Engineering Center, University of Southern California.

(1) Introduction

SINCE ITS INCEPTION by Prandtl in 1904, boundary-layer theory has become a highly developed and important branch of fluid mechanics. There are, however, a number of viscous flow problems which do not fit within the framework of Prandtl boundary-layer theory; one of these is the flow of a viscous fluid at low or moderate Reynolds numbers in closed channels or ducts. At high Reynolds numbers the viscous effects in closed channels are limited to a thin layer next to the wall and boundary-layer theory may be applied with good accuracy. At moderate or low Reynolds numbers the viscous effects may extend throughout the entire flow field and the assumption of a thin viscous layer with an essentially inviscid main flow is violated.

While viscous low Reynolds number flow in closed channels is related to the boundary-layer problem it has not undergone the same degree of development. There are, of course, a few exact solutions for flows in closed channels, notably Hagen-Poiseuille flow and the solution for incompressible flow between convergent or divergent plane walls. There exists also a number of

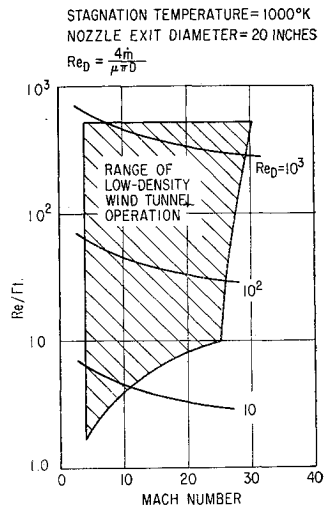

FIG. 1. Reynolds numbers for low density wind-tunnel operation.

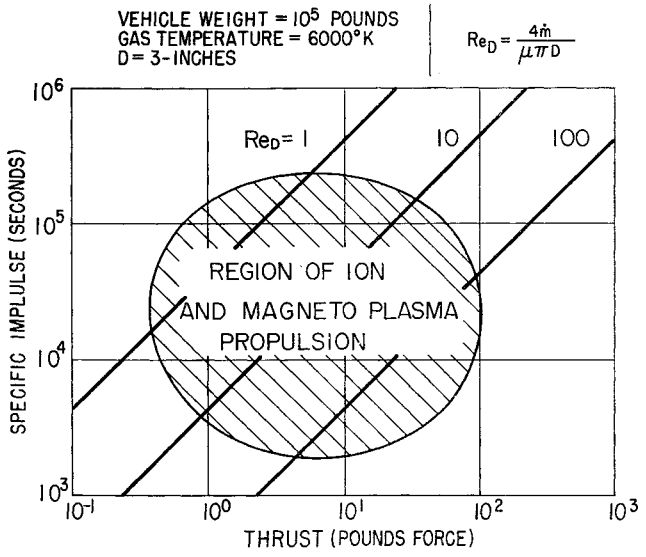

FIG. 2. Reynolds numbers for ion and magneto-plasma propulsion.

approximate solutions[1–6] for flows in closed channels. The number of such solutions is relatively small because of the lack of any large-scale interest in these problems. The number of solutions which include compressibility effects is extremely small because of the mathematical difficulties involved when the assumption of incompressibility is removed.

Recent advances in aerodynamics and space technology have brought to light two new areas in which compressible viscous channel flows will play an important role. These are: (1) the flow in the nozzle of a low-density hypersonic wind tunnel and (2) the flow through arc jet or magnetohydrodynamic propulsion systems used for space flight. Fig. 1 shows in the Mach number-Reynolds number plane the region in which low-density hypersonic wind tunnels are expected to operate.[7] Fig. 2 shows the region of operation of arc jet and magnetohydrodynamic propulsion systems associated with space propulsion of a 100,000-lb vehicle.[8] Superimposed on these figures are lines of constant Reynolds number (Reynolds number based on mass flow and characteristic diameter). It is clear from the Reynolds numbers involved that viscous effects will play an important role in the flow through each of these devices.

This then is the reason for renewed interest in the field of compressible viscous flow in closed channels. In the present paper an attempt is made to yield some insight into the problem by obtaining exact solutions to the approximate equations of motion valid for viscous compressible and incompressible flow in slender channels.

(2) Approximate Equations of Motion

The problem at hand is to determine the motion of a viscous, compressible, heat-conducting gas in a channel bounded by two walls (two-dimensional channel), or by a surface of revolution (axisymmetric channel). The flow configurations are shown in Fig. 3. The motion of such a gas is governed by the Navier-Stokes Equations. In most practical cases the channels under consideration are slender—i.e., the length of the channel, l is much greater than the radius (or half height) r—so that $r \ll l$. The approximate equations of motion describing the flow in slender channels at moderate or high Reynolds numbers are identical in form with the boundary-layer equations. This fact was alluded to in Ref. 6. The detailed order of magnitude analysis which leads to this conclusion was carried out in Ref. 10.

For flow in slender channels then the approximate equations of motion for steady two-dimensional or axisymmetric flow are:

$$(\partial \rho u/\partial x) + (\partial \rho v/\partial y) + (\epsilon \rho v/y) = 0 \quad \text{continuity} \tag{1}$$

$$\rho u \frac{\partial u}{\partial x} + \rho v \frac{\partial u}{\partial y} + \frac{\partial p}{\partial x} = F_x + \frac{\partial}{\partial y}\left(\mu \frac{\partial u}{\partial y}\right) + \frac{\epsilon \mu}{y}\frac{\partial u}{\partial y} \quad x \text{ momentum equation} \tag{2}$$

$$\partial p/\partial y = F_y \quad y \text{ momentum equation} \tag{3}$$

$$\rho u\, cp \frac{\partial T}{\partial x} + \rho v\, cp \frac{\partial T}{\partial y} - u \frac{\partial p}{\partial x} = \frac{\partial}{\partial y}\left(k \frac{\partial T}{\partial y}\right) + \epsilon \frac{k}{y}\frac{\partial T}{\partial y} + \mu\left(\frac{\partial u}{\partial y}\right)^2 + Q \quad \text{energy equation} \tag{4}$$

$$p = \rho RT \quad \text{equation of state} \tag{5}$$

Here $\epsilon = 0$ for two-dimensional flow and $\epsilon = 1$ for axisymmetric flow. In writing the equations of motion it has been assumed that the gas is perfect and that the Stokes relation between the first and second viscosity coefficients is valid.

Although the equations of motion for flow in slender channels at moderate or high Reynolds numbers are identical in form with the boundary-layer equations, the present problem differs from the boundary-layer problem in two important respects. First, the pressure distribution in the thin boundary layer is generally known at the outset from a solution to the inviscid problem outside the boundary layer; in the channel-flow problem, the pressure distribution must be obtained as part of the solution. Second, the temperature and velocity are known at the upper edge of the boundary layer, again from a solution to the inviscid problem, and may be used as boundary conditions in the boundary-layer problem; in the channel-flow problem, velocity and temperature distributions are not known in any part of the flow field so that other boundary conditions must be sought. If the channel is symmetric or axisymmetric, then the transverse velocity and the transverse gradient of the longitudinal velocity must vanish at the centerline from symmetry considerations. Also, if the channel walls are impermeable, the total mass-flow rate through the channel must be constant. These then are the boundary

conditions which must be used in the channel-flow problem.

(3) Incompressible Flow

The fact that the equations of motion for flow in slender channels are identical in form with the boundary-layer equations suggests the possibility of employing the mathematical techniques of boundary-layer theory in solving the channel-flow problem. In this section the method of similar solutions will be used to obtain solutions to the problem of incompressible viscous flow in slender channels. Solutions are found for both two-dimensional and axisymmetric flows, but consideration is limited to flows with no body force.

For incompressible flows with no body force, Eqs. (1), (2), and (3) become

$$(\partial u/\partial x) + (\partial v/\partial y) + \epsilon(v/y) = 0 \tag{1a}$$

$$\rho u \frac{\partial u}{\partial x} + \rho v \frac{\partial u}{\partial y} + \frac{dp}{dx} = \mu \frac{\partial^2 u}{\partial y^2} + \epsilon \frac{\mu}{y} \frac{\partial u}{\partial y} \tag{2a}$$

$$\partial p/\partial y = 0 \tag{3a}$$

The boundary conditions are given by

$$u(x,r) = v(x,r) = 0$$
$$(\partial u/\partial y)(x,0) = v(x,0) = 0 \tag{6}$$

where r is the distance from the centerline of the channel to the walls. The condition of conservation of mass-flow rate is given by

$$\dot{m} = 2\pi^{\epsilon}\rho \int_0^r uy^{\epsilon}dy = \text{const.} \tag{7}$$

The continuity equation is satisfied identically by the introduction of the stream function defined by

$$u = (1/y^{\epsilon})(\partial\psi/\partial y); \quad v = -(1/y^{\epsilon})(\partial\psi/\partial x)$$

Now in a manner analogous to boundary-layer theory, a nondimensional stream function

$$f = \psi(x,y)/[(r^{3+\epsilon}/\mu)(dp/dx)]$$

is introduced and the independent variables x and y are replaced by this new set

$$\xi = x/L, \quad \eta = y/r$$

In terms of the new stream function and the new coordinates, the longitudinal velocity component is:

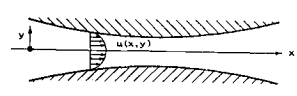

(A) FLOW IN A TWO-DIMENSIONAL CHANNEL.

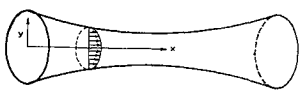

(B) FLOW IN AN AXISYMMETRIC CHANNEL.

FIG. 3. Geometries for flow in two-dimensional and axisymmetric channels.

$$u = (r^2/\eta^{\epsilon})(1/\mu)(dp/dx)(\partial f/\partial\eta) \tag{8}$$

and the condition of conservation of mass flow rate becomes

$$m = 2\pi \frac{\rho}{\mu} r^{3+\epsilon} \frac{dp}{dx} \int_0^1 \frac{\partial f}{\partial \eta} d\eta = \text{const.}$$

Since similar solutions are being sought it is anticipated that η will be the similarity variable. Thus f should be a function of η alone and it is clear from the condition of conservation of mass-flow rate that

$$(r^{3+\epsilon}/\mu)(dp/dx) = \alpha = \text{const.} \tag{9}$$

The normal component of velocity is given by

$$v = -\frac{\alpha}{y^{\epsilon}} \left\{ \frac{1}{L} \frac{\partial f}{\partial \xi} - \frac{\eta}{r} \frac{dr}{dx} \frac{\partial f}{\partial \eta} \right\} \tag{10}$$

Introducing the longitudinal and normal components of velocity and their derivatives into the equation, Eq. (2a) yields

$$\frac{\partial^2}{\partial \eta^2}\left(\frac{1}{\eta^{\epsilon}}\frac{\partial f}{\partial \eta}\right) + \frac{\epsilon}{\eta}\frac{\partial}{\partial \eta}\left(\frac{1}{\eta^{\epsilon}}\frac{\partial f}{\partial \eta}\right) - 1 + \frac{(1+\epsilon)}{\eta^{2\epsilon}} \frac{\rho\alpha}{r^{\epsilon}} \frac{1}{\mu} \frac{dr}{dx} \left(\frac{\partial f}{\partial \eta}\right)^2 = \frac{\rho\alpha}{\eta^{2\epsilon}} \frac{1}{r^{\epsilon}} \frac{1}{\mu} \times \left\{ \frac{r}{L} \frac{\partial f}{\partial \eta} \frac{\partial^2 f}{\partial \xi \partial \eta} + \left(\frac{\epsilon}{\eta} \frac{\partial f}{\partial \eta} - \frac{\partial^2 f}{\partial \eta^2} \right) \frac{r}{L} \frac{\partial f}{\partial \xi} \right\} \tag{11}$$

Now similar solutions exist only when f and $\partial f/\partial\eta$ do not depend upon ξ. Simultaneously the contraction $\frac{\rho\alpha}{\mu^{\epsilon} r} \frac{dr}{dx}$ must be independent of x. Thus, for similar solutions to exist, the stream function $f(\eta)$ must satisfy the ordinary differential equation

$$\left(\frac{f'}{\eta^{\epsilon}}\right)'' + \frac{\epsilon}{\eta}\left(\frac{f'}{\eta^{\epsilon}}\right)' - 1 + \frac{(1+\epsilon)}{\eta^{2\epsilon}} \beta f'^2 = 0 \tag{12}$$

where the prime denotes differentiation with respect to η and

$$\beta = (\rho\alpha/\mu r^{\epsilon})(dr/dx) \tag{13}$$

is a constant.

(a) *Two-Dimensional Flow*

For two-dimensional flow $\epsilon = 0$ and the governing differential equation, Eq. (12), becomes

$$f''' - 1 + \beta f'^2 = 0 \tag{14}$$

where

$$\beta = (\rho\alpha/\mu)(dr/dx), \quad \alpha = (r^3/\mu)(dp/dx)$$

Thus for two-dimensional flow similar solutions are possible for convergent or divergent channels with plane walls. The boundary conditions applicable to Eq. (14) are:

$$f(0) = f''(0) = f'(1) = 0 \tag{15}$$

After introducing

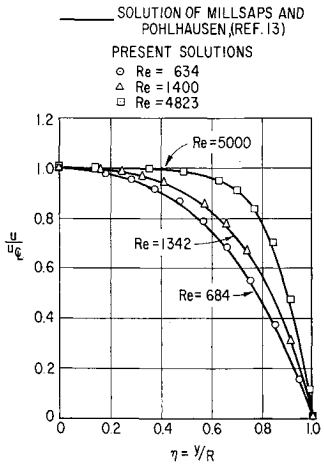

FIG. 4. Solutions for viscous incompressible flow in a convergent channel. (Wall angle = 5°.)

$$h^2 = 1 - [f'(\eta)/f'(0)]$$

Eq. (14) can be integrated twice to yield:

$$\sqrt{\pm\beta f'(0)/6}\,\eta = \int_0^h \frac{dh}{\sqrt{\pm\{h^4 - 3h^2 + 3(1 - [1/\beta f'(0)^2])\}}} \quad (16)$$

where the positive or negative sign is taken depending upon whether $\beta f'(0)$ is positive or negative respectively. The boundary condition $f''(0) = 0$ has been satisfied in writing Eq. (16). The right-hand side of (16) is a standard form of the well-known elliptic integrals[11] so that solutions may be obtained by employing tables of these integrals (e.g., Ref. 12). The remaining boundary condition $h(1) = 1, f'(1) = 0$ is satisfied if

$$\sqrt{\pm[\beta f'(0)/6]} = \int_0^1 \frac{dh}{\sqrt{\pm\{h^4 - 3h^2 + 3(1 - [1/\beta f'(0)^2])\}}} \quad (17)$$

Clearly there are only certain combinations of β and $f'(0)$ for which the solutions satisfy all the boundary conditions. The values of β and $f'(0)$ for which valid solutions are possible may be obtained by evaluating Eq. (17) for a number of assumed values of the parameter $\beta f'(0)^2$.

The exact form of the solution of Eq. (16) and the relationship between β and $f'(0)$ for which valid solutions are possible depends upon the signs of β and $f'(0)$ and upon the sign and magnitude of $\beta f'(0)^2$. Three classes of solutions are possible.

Class 1: $\beta > 0$, $f'(0) < 0$, $0 < \beta f'(0)^2 < 1$

The relationship between β and $f'(0)$ for which solutions are possible is

$$\sqrt{-[\beta f'(0)/6]} = m_1 F(\psi_1, k_1)$$

and the solution is given by

$$h^2 = b_1^2 k_1^2\, sd\{(1/m_1)\sqrt{-[\beta f'(0)/6]}\eta, k_1\}$$

where

$$a_1^2 = (3/2)[1 + \sqrt{1 + (4/9)\phi_1}]$$

$$b_1^2 = -(3/2)[1 - \sqrt{1 + (4/9)\phi_1}]$$

$$\phi_1 = -3\{1 - [1/\beta f'(0)^2]\} \quad k_1^2 = a_1^2/(a_1^2 + b_1^2),$$

$$m_1^2 = 1/(a_1^2 + b_1^2), \sin\psi_1 = \sqrt{(a_1^2 + b_1^2)/a_1^2(1 + b_1^2)}$$

Class 2: $\beta < 0$, $f'(0) < 0$, $\beta f'^2(0) < 0$

The relationship between β and $f'(0)$ for which solutions are possible is

$$\sqrt{\beta f'(0)/6} = m_2 F(\psi_2, k_2)$$

and the solution is given by

$$h^2 = a_2^2 b_2^2 \frac{\left\{1 - cn\left(\frac{1}{m_2}\sqrt{\frac{\beta f'(0)}{6}}\,\eta, k_2\right)\right\}}{1 + cn\left(\frac{1}{m_2}\sqrt{\frac{\beta f'(0)}{6}}\,\eta, k_2\right)}$$

where

$$a_2^2 = -(3/2)[1 + \sqrt{1 - (4/9)\phi_2}]$$

$$b_2^2 = -(3/2)[1 - \sqrt{1 - (4/9)\phi_2}]$$

$$\phi_2 = 3\{1 - [1/\beta f'(0)^2]\}$$

$$k_2^2 = -[(a_2 - b_2)^2/4\,a_2 b_2], \; m_2 = 1/2\sqrt{a_2 b_2}$$

$$\cos\psi_2 = (a_2 b_2 - 1)/(a_2 b_2 + 1)$$

Class 3a: $\beta > 0$, $f'(0) > 0$, $\beta f'(0)^2 > 4$.

The relationship between β and $f'(0)$ for which valid solutions are possible and the solution have the same form as Class 2.

Class 3b: $\beta > 0$, $f'(0) > 0$, $3 \leqslant \beta f'(0)^2 \leqslant 4$.

The relationship between β and $f'(0)$ for which valid solutions are possible is

$$\sqrt{\beta f'(0)/6} = m_3 F(\psi_3, k_3)$$

and the solution is given by

$$h^2 = b_3^2\, sn^2[(1/m_3)\sqrt{\beta f'(0)/6}\,\eta, k_3]$$

where

$$a_3 = (3/2)[1 + \sqrt{1 - (4/9)\phi_3}]$$

$$b_3 = (3/2)[1 - \sqrt{1 - (4/9)\phi_3}]$$

$$\phi_3 = 3\{1 - [1/\beta f'(0)^2]\}$$

$$k_3^2 = b_3^2/a_3^2, \; m_3 = 1/a_3^2, \; \sin\psi_3 = 1/b_3$$

No solutions are found with β negative and $f'(0)$ positive.

The type of physical solution obtained in each case depends upon the sign of β and $f'(0)$. Since the longitudinal velocity, $u = (\alpha/r)f'(\eta)$ is always positive, $f'(0)$ must have the same sign as α. Further, since

$$dr/dx = \beta\nu/\alpha \quad \text{and} \quad dp/dx = \alpha\mu/r^3$$

it is clear that Class 1 solutions correspond to flow in a convergent channel with negative pressure gradient.

Similarly, Class 2 solutions correspond to flow in a divergent channel with a negative pressure gradient, and Class 3 solutions correspond to flows in a divergent channel with a positive pressure gradient.

The solutions obtained here correspond to flows in convergent or divergent channels with plane walls. But these are just the flows for which exact solutions to the Navier-Stokes equations, in a polar coordinate system, are known. Thus very little new information is gained from these solutions. It is possible, however, to assess the validity of the approximate equations of motion by comparing the solutions obtained here with exact solutions for the same wall shapes. In Figs. 4 and 5 velocity profiles obtained by the present analysis for convergent and divergent channels of 5° half angle are compared with exact solutions as obtained by Millsaps and Pohlhausen.[13] The Reynolds number here is

$$Re = u_\ell r/\nu \tan\theta = \alpha f'(0)/\nu \tan\theta$$

which is the same as that used in Ref. 13. The Reynolds numbers for which the present solutions were computed were chosen so as to facilitate the use of the elliptic functions tables.[12] In all cases these Reynolds numbers are within 10 percent of the value for the corresponding exact solution. The close agreement between the solutions to the approximate equations of motion and the exact solutions leads one to conclude that the approximate equations of motion do accurately describe the flow in slender channels.

Two other points should be mentioned at this juncture. First, the two-dimensional Poiseuille flow, or "parallel" flow between parallel walls is included as a special case ($\beta = 0$) in the present solution. Second, the present analysis yields solutions for which the channel walls are divergent but the pressure gradient is negative (Class 2 above). Physically this solution corresponds to flows in a divergent channel at such low Reynolds numbers that the viscous layer on the wall builds up faster than the wall diverges. As a result, the flow near the centerline of the channel acts as if it were in a convergent channel.

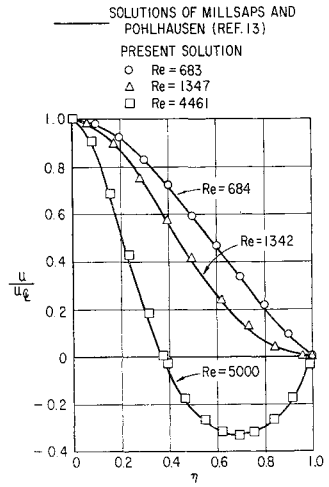

FIG. 5. Solutions for viscous incompressible flow in a divergent channel. (Wall angle = 5°.)

(b) Axisymmetric Flow

In the case of axisymmetric flow, the governing differential equation, Eq. (12), becomes

$$(f'/\eta)'' + (1/\eta)(f'/\eta)' - 1 + 2\beta(f'/\eta)^2 = 0 \quad (18)$$

where

$$\beta = (\rho\alpha/\mu r)(dr/dx), \quad \alpha = (r^4/\mu)(dp/dx)$$

Thus similar solutions are possible for wall shapes in which the wall radius varies exponentially with x—i.e.,

$$r \sim \exp \beta\nu x/\alpha$$

The boundary conditions applicable to Eq. (17) are

$$f'(1) = 0, f'(0) = 0, \lim_{\eta\to 0} \frac{f'}{\eta} \neq 0$$

$$\frac{\partial}{\partial\eta}\left(\frac{f'}{\eta}\right)\bigg|_{\eta=0} = 0$$

The differential equation can be put in a convenient form for solution by introducing

$$g(\eta) = f'(\eta)/\eta, \; g^* = g(\eta)/g(0)$$

and by changing the independent variable η to

$$\xi = \eta/\sqrt{\pm g(0)}$$

where the positive or negative sign is taken depending upon whether $g(0)$ is positive or negative respectively. In terms of g^* and ξ the differential equation becomes

$$d^2g^*/d\xi^2 = \pm(1 - 2\beta g^2(0)) - (1/\xi)(dg^*/d\xi) \quad (19)$$

The boundary conditions are

$$g^*(0) = 1, \quad (dg^*/d\xi)(0) = 0 \quad (20)$$

and from the differential equation

$$\frac{d^2g^*}{d\xi^2}\bigg|_{\xi=0} = \frac{1}{\xi}\frac{dg^*}{d\xi}\bigg|_{\xi=0} = \pm\frac{1}{2}\,1 - 2\beta\, g^2(0) \quad (21)$$

These equations were programmed for solution on an IBM 1620 computer for various values of the parameter $2\beta g^2(0)$. Every solution to Eq. (19) which satisfies the initial boundary condition, Eq. (20), is not necessarily a valid solution to the problem at hand. Only those solutions which cross the $g^* = 0$ axis satisfy the remaining boundary condition

$$f'(1) = 0 \text{ or } g^*(1/\sqrt{\pm g_0}) = 0$$

Again three classes of solutions are possible.

Class 1: $g(0) < 0, \beta > 0, 0 \leq 2\beta g(0)^2 \leq 1$

These solutions correspond to flows in convergent channels with negative pressure gradients.

Class 2: $g(0) < 0, \beta < 0, 2\beta g(0)^2 < 0$

These solutions correspond to flows in divergent channels with negative pressure gradients.

Class 3: $g(0) > 0$, $\beta > 0$, $2\beta g^2(0) > 8.6$.

These solutions correspond to flows in divergent channels with positive pressure gradients.

Velocity profiles for flow in convergent and divergent axisymmetric channels are presented in Figs. 6 and 7 respectively. In Fig. 7 the profile shown for a Reynolds number of 49 belongs to Class 2, the remaining profiles in Fig. 7 belong to Class 3 above.

Finally it is observed that the well-known Hagen-Poiseuille solution for flow in a straight pipe is included as a special case ($\beta = 0$) in the axisymmetric flow solutions.

(4) Compressible Flow

Compressible viscous flow in slender two-dimensional channels will now be studied. In this analysis it is assumed that there are no body forces, no internal heat addition, Q, that the gas is perfect and has a constant specific heat cp, that the Prandtl number is unity, that the viscosity temperature relationship is linear—i.e., $\mu = \mu_0 T/T_0$—and that the wall is insulated.

Under the conditions specified above the energy equation has the simple solution

$$cp\ T + (u^2/2) = cp\ T_0 = \text{const.} \tag{22}$$

and the flow is isoenergetic. The compressible viscous flow problem may be transformed into an equivalent incompressible problem by employing a Stewartson-type transformation in which the independent variables x and y are replaced by the new set X and Y defined by

$$X = \int_0^x \frac{p}{p_0}\,dx, \quad Y = \int_0^y \frac{\rho}{\rho_0}\,dy \tag{23}$$

Introducing a new set of velocity components defined by

$$U = \partial\psi/\partial Y, \quad V = -\partial\psi/\partial X$$

where ψ is the proper stream function in the physical coordinate system, the equations of motion become

$$(\partial U/\partial X) + (\partial V/\partial Y) = 0 \tag{24}$$

$$U\frac{\partial U}{\partial X} + V\frac{\partial U}{\partial Y} + \frac{1}{\rho}\frac{\partial p}{\partial X} = \nu_0\frac{\partial^2 U}{\partial Y^2} \tag{25}$$

$$\partial p/\partial Y = 0 \tag{26}$$

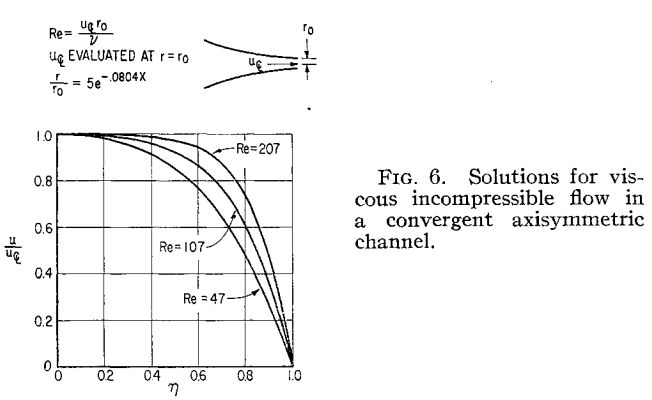

FIG. 6. Solutions for viscous incompressible flow in a convergent axisymmetric channel.

The density is eliminated from Eq. (25) by employing the equation of state and the energy integral, Eq. (22). Upon elimination of the density, Eq. (25) becomes

$$U\frac{\partial U}{\partial X} + V\frac{\partial U}{\partial Y} + \Re\left(T_0 - \frac{U^2}{2cp}\right)\frac{d\ln p}{dX} = \nu_0\frac{\partial^2 U}{\partial Y^2} \tag{27}$$

The boundary conditions in the transformed coordinate system are

$$U(X,R) = V(X,R) = 0$$
$$(\partial U/\partial Y)(X,0) = V(X,0) = 0$$

where

$$R = \int_0^r \frac{\rho}{\rho_0}\,dy$$

If, by analogy with the incompressible problem, one now introduces the nondimensional stream function

$$f(\xi,\eta) = [\psi(XY)/(\Re T_0/\nu_0)R^3(d\ln p/dX)]$$

and the nondimensional coordinates

$$\xi = X/L, \quad \eta = Y/R$$

the longitudinal velocity component becomes

$$U(X,Y) = \frac{\Re T_0 R^2}{\nu_0}\frac{d\ln p}{dx}\frac{\partial f}{\partial \eta}$$

From the condition of conservation of mass flow in the channel it is found that

$$\frac{\Re T_0}{\nu_0}R^3\frac{d\ln p}{dX} = \alpha = \text{const.} \tag{28}$$

Finally, if one seeks similar solutions, it is found that for similar solutions to exist the stream function, $f(\eta)$, must satisfy the ordinary differential equation

$$f''' - 1 + \beta f'^2 = 0 \tag{29}$$

where the prime denotes differentiation with respect to η and β is the constant

$$\beta = \frac{\alpha^2}{2cp\ R^2\ T_0} + \frac{\alpha}{\nu_0}\frac{dR}{dX}$$

The boundary conditions applicable to Eq. (29) are

$$f(0) = f''(0) = f'(1) = 0 \tag{30}$$

The governing equation for the nondimensional stream function, Eq. (29), and the boundary conditions, Eq. (30), are the same as the governing equation, Eq. (14), and boundary conditions, Eq. (15), for the nondimensional stream function in incompressible flow. Thus the solutions obtained in Section (3a) may be used directly to determine the flow of a compressible gas in a two-dimensional channel. One must now make the inverse transformation from the transformed coordinates, X and Y, to the physical coordinates, x and y, to determine the wall shapes for which solutions are possible in the compressible problem.

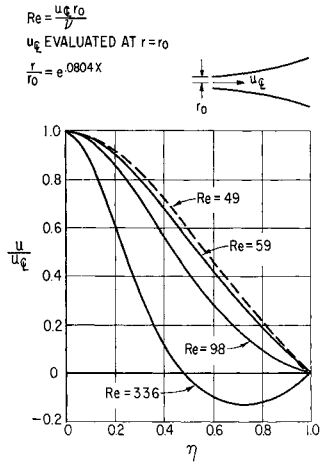

FIG. 7. Solutions for viscous incompressible flow in a divergent axisymmetric channel.

Similar solutions are possible for wall shapes (in the transformed coordinates) which are defined by

$$dR^*/dX = b[1 - (a/R^{*2})] \tag{31}$$

and for pressure distribution defined by

$$\frac{1}{p^*}\frac{dp^*}{dX} = \frac{2\gamma\, ab}{(\gamma - 1)R^{*3}} \tag{32}$$

where $R^* = R/R_1$, $p^* = p/p_1$, $a = \alpha^2/2cp\ T_0R_1^2\beta$, and $b = \nu_0\beta/\alpha R_1$. Combining Eqs. (31) and (32) and integrating yields

$$p^* = \left\{\frac{R^{*2} - a}{R^{*2}(1 - a)}\right\}^{\gamma/(\gamma-1)} \tag{33}$$

The relationships between the natural and the transformed coordinates are obtained by inverting the transformation relations given by Eq. (23). Employing (23) and (31) the physical x-coordinate becomes

$$x = \frac{p_0}{p_1}(1 - a)^{\gamma/(\gamma-1)} \int_0^{R^*} \left(\frac{R^{*2}}{R^{*2} - a}\right)^{(2\gamma-1)/(\gamma-1)} dR^*$$

which for $\gamma = 1.4$ can be integrated directly to yield

$$\frac{xb}{(1 - a)^{\gamma/(\gamma-1)}}\frac{p_1}{p_0} = \frac{\sqrt{R^{*2} - a}}{7}\left\{\frac{128}{5} - \frac{64}{5}\frac{R^{*2}}{R^{*2} - a} - \frac{16}{5}\left(\frac{R^{*2}}{R^{*2} - a}\right)^2 - \frac{8}{5}\left(\frac{R^{*2}}{R^{*2} - a}\right)^3 - \left(\frac{R^{*2}}{R^{*2} - a}\right)^4\right\} + \text{const.} \tag{34}$$

where the constant is evaluated so that $x = 0$ at $R^* = 1$.

Making use of the energy integral to eliminate the density, the physical y-coordinate becomes

$$y = \frac{p_0}{p}\frac{1}{p^*}\int_0^\eta \left(1 - \frac{a\beta f'^2}{R^{*2}}\right) d\eta$$

or when the differential equation, Eq. (29), is used

$$y = \frac{p_0}{p_1} R_1 \frac{R^*}{p^*}\int_0^\eta \left(1 - \frac{a}{R^{*2}} + \frac{af'''}{R^{*2}}\right) d\eta$$

Integration yields

$$\frac{y}{R_1} = \frac{p_0}{p_1}\frac{R^*}{p^*}\left\{\left(\frac{R^{*2} - a}{R^{*2}}\right)\eta + \frac{a}{R^{*2}} f''(\eta)\right. \tag{35}$$

since $f''(0) = 0$. The wall coordinate is obtained when $\eta = 1$ so that

$$\frac{r}{R_1} = \frac{p_0}{p_1}\frac{R^*}{p^*}\left\{\frac{R^{*2} - a}{R^{*2}} - \frac{a}{R^{*2}} f''(1)\right\} \tag{36}$$

Since the wall coordinate r depends upon $f'(1)$, it is obvious that each solution to the basic differential equation, Eq. (29), corresponds to flow in a channel of different wall shape. Thus it is not possible to find solutions for a fixed wall shape over a complete range of Reynolds numbers. It is possible, however, to study the general characteristics of viscous compressible flows with the solution obtained here.

As a result of the Stewartson-type transformation and the similarity transformation, the compressible problem is reduced to that of solving the equivalent incompressible problem. Thus, as in the incompressible case, three classes of solutions are found. In the compressible flow problem the three classes of solutions given in Section (3a) have the following physical characteristics.

Class I: Solutions of Class I correspond to flows with a negative pressure gradient in convergent channels with a throat for small values of a and in divergent channels for larger values of the parameter a.

Class II: Solutions of Class II correspond to flows with a negative pressure gradient in divergent channels.

Class III: Solutions of Class III correspond to flows with positive pressure gradients in divergent channels for small values of a and in convergent channels for larger values of a.

A preliminary study of the solutions of Class II indicates that the scaling parameter b takes on unreasonable values unless the Mach number is small—i.e., the flow is essentially incompressible. Thus flows of Class II are excluded from further consideration here.

A typical solution of Class III has been computed for the case where $a = 0.1$, $\beta f'(0)^2 = 3.89$ ($\beta = 467$, $f'(0) = 0.0913$), $p_0 = 10^{-3}$ atmospheres, $T_0 = 800°$K and $r(x = 0) = 5$ cm. These conditions correspond to an initial Mach number of 1.78 and a Reynolds number ($u_\ell r/\nu_0$, where u_L and r are evaluated at $x = 0$) of 484. The wall shape and several constant Mach number contours for this flow field are shown in Fig 8. This flow field is interesting since it shows a reversal of the flow next to the wall similar to that found in the incompressible solution (as for example Fig 5). The extent of this reverse flow region is shown in Fig. 8 where the zero Mach number contour represents the boundary between the main flow and the reverse flow regions. In the region between the contour $M = 0$ and the wall, the Mach number is negative indicating negative (reverse) velocity.

Perhaps the most interesting of the three classes of solutions is Class I which yields flows in convergent-

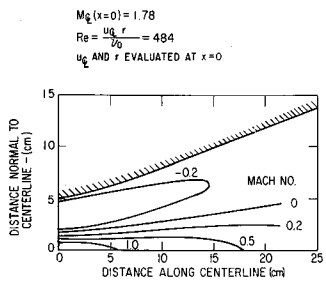

FIG. 8. Wall shape and constant Mach number contours for compressible flow in a divergent channel.

divergent channels with a negative pressure gradient. This type of flow is found in supersonic wind tunnel nozzles, jet and rocket engine nozzles, and many flow-metering devices. A typical solution of this class has been computed for the case where $a = 10^{-3}$, $\beta f'(0)^2 = 0.9772$ ($\beta = 205.3$, $f'(0) = -0.06896$), $p_0 = 10^{-3}$ atm, $T_0 = 400°$K and $r(x = 0) = 5$ cm. This corresponds to a flow in a convergent-divergent channel with an initial Mach number of 0.07 and a Reynolds number (based on mass flow per unit channel width) of 87.3. The wall shape, pressure distribution, and centerline Mach number for this solution is presented in Fig. 9. Fig 10 presents a detailed Mach number distribution in the immediate vicinity of the channel throat. It is here that the viscous effects are most striking. An inviscid one-dimensional analysis of the flow in a convergent-divergent channel with a negative pressure gradient leads to the result that the Mach number at the geometric throat can only be unity, and the pressure ratio at the throat, $(p/p_0)_t$, must therefore be $[2/(\gamma + 1)]^{\gamma/(\gamma-1)} = 0.5283$ for air ($\gamma = 1.4$). If viscous effects are large, however, this is not true. In Fig. 10, constant Mach number contours are shown for Mach numbers of 0.7, 0.8, 0.9, and 1.0 (sonic line). It is clear that one of the effects of viscosity is to transpose the sonic line (and all other constant Mach number lines) downstream of the geometric throat and to cause the sonic line to curve into the divergent portion of the channel. The transposing of the sonic line downstream of the geometric throat is due to the displacement effect of the viscous layer near the wall. One might wish to define an effective inviscid channel width by subtracting from the actual channel width twice the displacement thickness $\delta^* = \int_0^r \left(1 - \frac{\rho u}{\rho_c u_c}\right) dy$. The approximate location of the sonic line would then be given by the point at which $d\bar{A}/dx = 0$, where $\bar{A}$ is the effective channel width (area).

If the sonic line lies downstream of the geometric throat, then the pressure ratio should be greater than the value $[2/(\gamma + 1)]^{\gamma/(\gamma-1)}$ predicted by inviscid theory. An approximate relationship between the pressure at the geometric throat and the Reynolds number may be obtained from the present analysis. The location of the geometric throat for solutions of Class I may be found by differentiating Eq. (36) with respect to x and setting the result equal to zero. In this manner it is found that the value of R^{*2} corresponding to the geometric throat is

$$R_t^{*2} = a\left\{1 + \frac{1}{2}\left(\frac{2}{\gamma - 1} + f''(1)\right) + \frac{1}{2}\sqrt{\left[\frac{2}{\gamma - 1} + f''(1)\right]^2 + \frac{8\gamma f''(1)}{\gamma - 1}}\right.$$

The pressure ratio at the geometric throat is given

$$\left(\frac{p}{p_0}\right)_t = \left[\frac{R_t^{*2} - a}{R_t^{*2}(1 - a)}\right]^{\gamma/(\gamma-1)} \frac{p_1}{p_0}$$

If a is assumed to be much smaller than unity, then the initial Mach number is small and $p_1/p_0 = 1$. Neglecting a compared to unity, the pressure ratio at the geometric throat becomes

$$\left(\frac{p}{p_0}\right)_t = \left\{\frac{\frac{2}{\gamma + 1} + f''(1) + \sqrt{\left[\frac{2}{\gamma + 1} + f''(1)\right]^2 + \frac{8\gamma f''(1)}{\gamma - 1}}}{2 + \frac{2}{\gamma + 1} + f''(1) + \sqrt{\left[\frac{2}{\gamma + 1} + f''(1)\right]^2 + \frac{8\gamma f''(1)}{\gamma - 1}}}\right\} \tag{37}$$

The mass flow per unit width of the channel is $\dot{m} = 2\rho_0 \alpha f(1)$ so the Reynolds number based on mass flow is

$$Re = \frac{\dot{m}}{\mu_0} = \frac{2\alpha f(1)}{\nu_0} = \frac{2\beta f(1)}{bR_1} \tag{38}$$

Now b and R_1 are scale factors determining the size of the channel involved. Since each solution corresponds to a channel of slightly different geometry, it is impossible to determine the effects of viscosity on a single geometry over a large range of Reynolds numbers. For this reason it is convenient to ignore the scaling factor bR_1 and take the parameter $\beta f(1)$ as representative of Reynolds number.

The pressure ratio at the geometric throat is presented as a function of $\beta f(1)$ in Fig. 11. Inspection of Fig 11 shows that as the Reynolds number $[\beta f(1)]$ is decreased, the pressure ratio at the geometric throat rises above its inviscid ($Re = \infty$) value of 0.528.

In addition to predicting the rise in throat pressure ratios resulting from viscous effects, it is also possible to show, with the present analysis, the effect of Reynolds number on the discharge coefficient of a convergent-divergent channel. The discharge coefficient is defined as the ratio of the actual mass flow which passes through a given nozzle to the ideal mass flow which would pass through the same nozzle at the same pressure ratio. From the present analysis, the actual mass flow which passes through the nozzle is given by

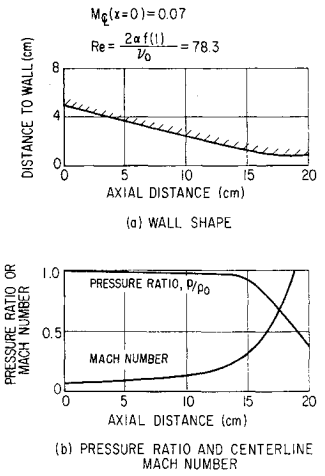

FIG. 9. Wall shape, centerline Mach number, and pressure distribution in a convergent-divergent channel.

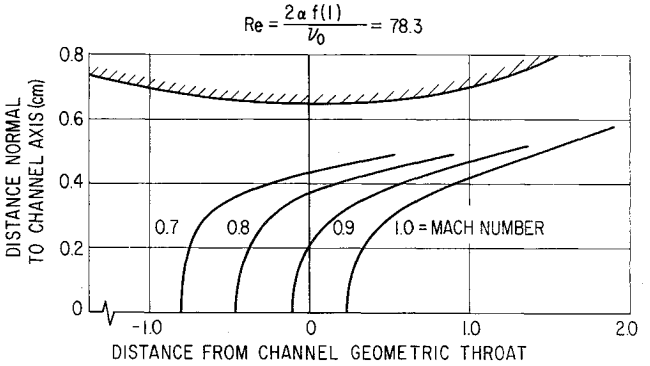

FIG. 10. Constant Mach number profiles near the throat of a convergent-divergent channel.

Eq. (38). The ideal mass flow which would pass through the same nozzle at the throat pressure ratio $(p/p_0)_t$ is:

$$\dot{m}_t = 2\rho_0 r_t \sqrt{\Re T_0}\sqrt{\frac{2\gamma}{\gamma-1}\left(\frac{p}{p_0}\right)_t^{(\gamma+1)/\gamma}\left[\left(\frac{p}{p_0}\right)_t^{(1+\gamma)/\gamma}-1\right]}$$

The discharge coefficient therefore is given by

$$C_D = \frac{\sqrt{a\beta f(1)}}{\frac{r_t}{R_1}\left(\frac{p}{p_0}\right)_t^{(\gamma+1)/\gamma}\left[\left(\frac{p}{p_0}\right)_t^{(1-\gamma)/\gamma}-1\right]}$$

where

$$\frac{r_t}{R_1} = \frac{R_t^*}{p_t^*}\left[\frac{R_t^{*2}-a}{R_t^{*2}}+\frac{af''(1)}{R_t^{*2}}\right]$$

The discharge coefficient has been computed from these equations using the solutions of Class I and is presented in Fig. 12 as a function of $\beta f(1)$ which is representative of Reynolds number. It is, of course, not surprising to find that the discharge coefficient decreases as the Reynolds number decreases.

(5) Concluding Remarks

Similar solutions to the approximate equations of motion valid for moderate or high Reynolds number flows in slender channels have been obtained for incompressible two-dimensional and axisymmetric flows and for compressible flows through two-dimensional channels with adiabatic walls.

It was found that similar solutions in the incompressible two-dimensional problem are possible for flows in convergent or divergent channels with plane walls. By comparing these solutions with exact solutions to the Navier-Stokes equations for the same problem, one is able to show that the approximate equations of motion do accurately describe the flow in slender channels.

In the case of incompressible-axisymmetric flow, similar solutions are possible for flow in channels where the wall radius varies exponentially with the distance along the channel. For this type of flow the pressure gradient is inversely proportional to the fourth power of the wall radius.

In the case of compressible flow through two-dimensional channels with adiabatic walls, similar solutions are possible for a variety of wall shapes. A study of compressible flows in convergent-divergent channels indicates that:

(1) As a result of viscous effects in the channel the sonic line lies downstream of the channel geometric throat.

(2) The pressure ratio at the geometric throat is greater than the value predicted by inviscid theory, and increases as the Reynolds number is decreased.

(3) The discharge coefficient for the channel decreases as the Reynolds number is decreased. A plot of discharge coefficient as a function of Reynolds number resembles very closely similar curves for incompressible flow.

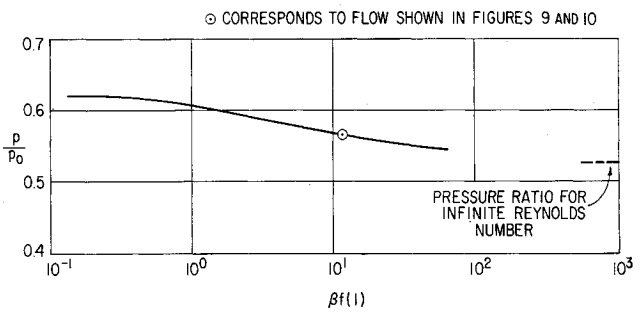

FIG. 11. Effect of viscosity on the pressure ratio at the throat of a convergent-divergent channel.

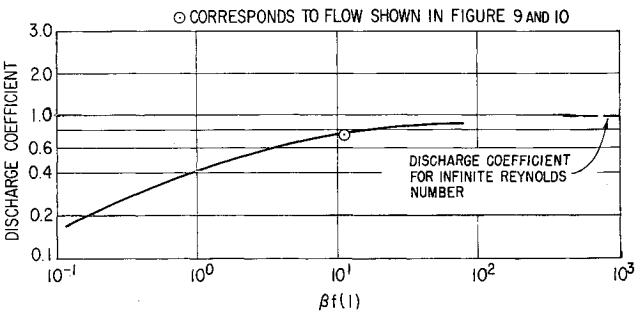

FIG. 12. Effect of viscosity on the discharge coefficient for compressible flow in a convergent-divergent channel.

References

[1] Schiller, L., *Die Entwicklung der Laminaren Geschwindigkeitsverterterlung und ihre Bedentung fur Zahigkeitsmessungen*, ZAMM, Vol. 2, p. 96, 1922.

[2] Boussinesq, J., *Sur la maniere dont les vitesses, dous un tube cylandrique de section circulaire, evase a son entrec, se distribuent depuis celle entric jusqn' aus endroits au trouve etabli un regime uniforme*, Comptes Rendus, Vol. 113, pp. 9–15, 49–51, 1891.

[3] Rivas, Miguel A., Jr., and Shapiro, Ascher H., *On the Theory of Discharge Coefficients for Round-Entrance Flowmeters and Venturis*, Trans. ASME, Vol. 78, No. 3, pp. 489–497, April 1956.

[4] Simmons, Frederick S., *Analytical Determination of Discharge Coefficients for Flow Nozzles*, NACA TN 3449, 1955.

[5] Maslen, Stephen H., *On Fully Developed Channel Flows: Some Solutions and Limitations, and Effects of Compressibility, Variable Properties, and Body Forces*, NASA TR R-34, 1959.

[6] Martin, Dale E., *A Study of Laminar Compressible Viscous Pipe Flow Accelerated by a Body Force, with Application to Magnetogasdynamics*, NASA TN D855, April 1961.

[7] Henshal, Brian D., and Zlotnic, Martin, *Design Study for a Hypersonic Low Density Wind Tunnel*, Research and Advanced Development Div., Avco Corp., Tech. Rep., RAD-TR-9-60-37, Jan. 31, 1961.

[8] Sutton, George P., *Rocket Propulsion Systems for Interplanetary Flight*, Journal of the Aero/Space Sciences, Vol. 26, No. 10, Oct. 1959.

[9] Pai, Shih I., *Viscous Flow Theory, Volume 1 Laminar Flow*, 1st Ed., D. Van Nostrand Company, Inc., Princeton, N. J., 1956.

[10] Williams, James C. III, *A Study of Compressible and Incompressible Viscous Flow in Slender Channels*, Ph.D. Thesis, University of Southern California, June 1962.

[11] Byrd, Paul F., and Friedman, Morris D., *Handbook of Elliptic Integrals for Engineers and Physicists*, Springer-Verlag, Berlin, 1954.

[12] Spencley, G. W., and Spencley, R. M., *Smithsonian Elliptic Functions Tables*, Smithsonian Institution, Washington, D. C., Nov. 1, 1947.

[13] Millsaps, Knox, and Pohlhausen, Karl, *Thermal Distribution in Jeffery-Hamel Flows Between Nonparallel Plane Walls*, Journal of the Aeronautical Sciences, Vol. 20, No. 3, March 1953.

✦ ✦ ✦

Slender Shapes of Minimum Drag

(*Continued from page 178*)

[5] Cole, J. D., *Newtonian Flow Theory for Slender Bodies*, Journal of the Aeronautical Sciences, Vol. 24, No. 6, June 1957.

[5] Hayes, W. D. and Probstein, R. F., *Hypersonic Flow Theory*, Academic Press, New York, 1959.

[7] Chernyi, G. G., *Introduction to Hypersonic Flow*, Academic Press, New York, 1961.

[8] Gonor, A. L., *Determination of the Shape of a Body of Minimum Drag at Hypersonic Speed*, PMM, Vol. 24, No. 6, 1960.

[9] Bliss, G. A., *Lectures on the Calculus of Variations*, The University of Chicago Press, Chicago, 1946.

[10] Miele, A., *The Calculus of Variations in Applied Aerodynamics and Flight Mechanics*, Boeing Scientific Research Labs., Flight Sciences Lab., TR No. 41, 1961.

[11] Miele, A., (Editor), *Extremal Problems in Aerodynamics*, Academic Press, New York, 1963.

✦ ✦ ✦